Scripta Materialia 230 (2023) 115405

Contents lists available at ScienceDirect

Scripta Materialia

journal homepage: www.journals.elsevier.com/scripta-materialia

Energy dissipation by grain boundary replacement during grain growth

Zipeng Xu [a], Christopher M. Hefferan [b], Shiu Fai Li [b], Jonathan Lind [b], Robert M. Suter [b], Fadi Abdeljawad [c,d], Gregory S. Rohrer [a,*]

[a] Department of Materials Science and Engineering, Carnegie Mellon University, Pittsburgh, PA 15213, United States of America
[b] Department of Physics, Carnegie Mellon University, Pittsburgh, PA 15213, United States of America
[c] Department of Mechanical Engineering, Clemson University, Clemson, SC 29634, United States of America
[d] Department of Materials Science and Engineering, Clemson University, Clemson, SC 29634, United States of America

A B S T R A C T

The changes in both the grain boundary area and grain boundary energy that occur during grain growth have been measured in polycrystalline Ni using high energy diffraction microscopy. In addition to the reduction of grain boundary area, the average grain boundary energy decreases as higher energy grain boundaries are replaced by lower energy grain boundaries. This energy dissipation mechanism influences grain boundary migration and might explain the absence of a correlation between grain boundary curvature and migration velocity.

Classical studies of isotropic grain growth in polycrystals have been based on the idea that grain boundary (GB) migration is driven by the product of the GB energy and curvature. [1,2] While support for this foundational concept is certainly found in studies of bicrystals [3] and simulations [4], recent experimental evidence contradicts this idea. When measured curvatures and velocities were compared in Ni [5] and $SrTiO_3$, [6] they were found to be uncorrelated. Similar observations were reported for α-Fe, [7] where the measured constant of proportionality between curvature and velocity did not behave in expected ways. The purpose of this letter is to present evidence that, during grain growth, the replacement of higher energy GBs by lower energy boundaries dissipates energy by a mechanism that is not related to curvature. This reduction of the average GB energy represents an additional driving force for grain growth.

For a GB network comprised of N triangular mesh elements of area a_i, the total free energy (F) is:

$$F = \sum_{i=1}^{N} \gamma(p_5) a_i \tag{1}$$

Where $\gamma(p_5)$ is the five-parameter GB energy function that depends on GB misorientation and GB inclination and p_5 is a vector specifying the five GB parameters. If, during grain growth, GB area is eliminated randomly and the GB character distribution remains constant, then the average GB energy, $\gamma=\langle\gamma(p_5)\rangle$, will not change. However, if the GB distribution changes, so will the average GB energy. While Eq. (1) is used for calculations in this paper, for the next stage of discussion we simplify it to $F=\gamma A$ where A is the total area and γ is the average GB energy. In the absence of stored plastic energy or external forces, the free energy can decrease with time (t) by both the reduction in the total area and by changes in the GB character distribution that reduce the average GB energy. The derivative of the energy with respect to time gives the energy dissipated during annealing:

$$\frac{dF}{dt} = \gamma\frac{dA}{dt} + A\frac{d\gamma}{dt} < 0 \tag{2}$$

Classically, only the first term in the derivative ($\gamma\frac{dA}{dt}$) is considered. In this case, the energy dissipation must be manifest as a decrease in the area and an increase in the average grain size. [8] If the GB free energy is reduced only by the reduction of the area, then it is predicted that all boundaries should move toward their centers of curvature. [1,9,10] However, it is only valid to ignore the second term of Eq. (2) in the special case where the average GB energy is constant with time ($\frac{d\gamma}{dt} = 0$). While the energy per area of any specific GB with a constant misorientation and GB normal is not expected to change with time, the distribution of GB types can change with time. In real polycrystals with anisotropic GB energies, when the types of GBs in the population change with time, the average energy can also change with time. In the case that $\frac{d\gamma}{dt}$ is negative, it is not necessary for $\frac{dA}{dt}$ in Eq. (2) to be negative, so GBs will not necessarily migrate towards their centers of curvatures as normally assumed.

The idea that the average GB energy can decrease with time through changes in the GB character distribution has been proposed in the past [11–16], but not directly measured. Precedents for the reduction of GB energy by changes in the GB character distribution are found in the well-known phenomena of GB faceting [17–23] and corner twin growth

* Corresponding author.
E-mail address: gr20@andrew.cmu.edu (G.S. Rohrer).

https://doi.org/10.1016/j.scriptamat.2023.115405
Received 11 January 2023; Received in revised form 28 February 2023; Accepted 4 March 2023

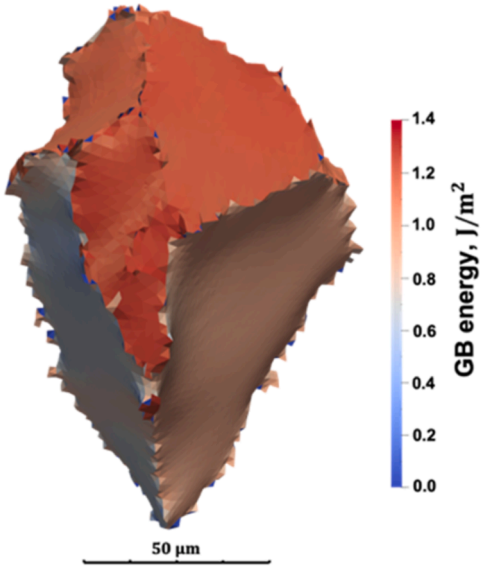

Fig. 1. A grain within polycrystalline Ni. The GBs are approximated by a triangular mesh and each triangle is colored according to the energies assigned by the BRK function.

[24–27], where a positive $\frac{dA}{dt}$ is compensated by a negative $\frac{d\gamma}{dt}$. Cahn and Hoffman [28,29] formulated the capillarity vector in part to describe the fact that it is possible to reduce energy through interface reorientation – as happens during faceting.

Here we present evidence that during grain growth, the average GB energy decreases as higher energy GBs are eliminated, thus altering the driving force for GB migration. This reduction in average GB energy is possible because there is a spectrum of GB energies and, in sufficiently large samples, the boundaries occupy the full range of this spectrum. [30] The purpose of this letter is to show that during grain growth, the GB distribution evolves, resulting in a decrease in the average GB energy through an increase in the relative areas of the lower energy GBs and a decrease in the relative areas of the high energy boundaries. Here we experimentally quantify this energy decrease. This is important because it influences the direction and speed of GB migration. Importantly, the driving force that derives from lowering the average GB energy will drive boundaries in directions unrelated to curvature and this provides a plausible explanation for recent experimental results showing no correlation between curvature and migration velocity. [5,6]

To quantify the change in the GB energy with time during grain growth, we use the microstructure of high purity Ni that was imaged by high energy diffraction microscopy (HEDM) at six times during an interrupted annealing experiment. The stress-free sample was annealed at roughly 30 min intervals at 800 °C. During this time, the mean grain size (spherical equivalent radius) increased from 19 μm to 23 μm. These data have been the subject of other analyses and the details of the experiment and acquisition of the data are available in earlier publications. [5,31,32] In [5], the microstructures were reconstructed with a voxel resolution of $2.8 \times 2.8 \times 4.0\ \mu m$ and the GBs were approximated by a triangular mesh constructed in DREAM.3D, [33] as described previously. At the end of this process, the five GB bicrystal parameters for each triangular mesh element of more than 50,000 boundaries were defined.

An energy was assigned to each triangular mesh element using the function defined by Bulatov et al. [34], referred to here as the Bulatov-Reed-Kumar (BRK) function. The function was defined by fitting curves to a large set of GB energies calculated by molecular dynamics (MD). [35] While the BRK energies are clearly an approximation of the true energies, the MD calculated energies on which they are based have been shown to be correlated with experimentally determined

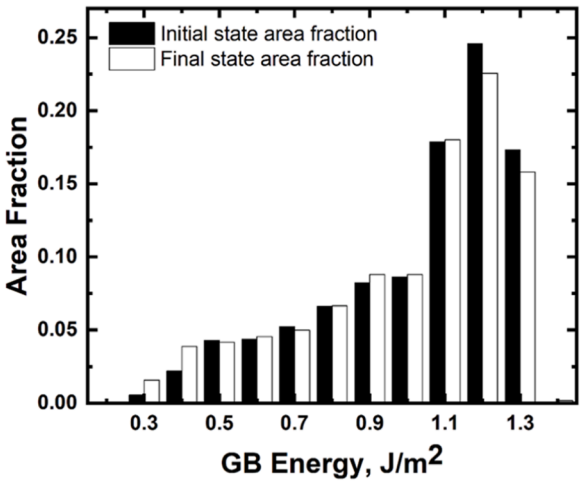

Fig. 2. Distribution of GB energies in the initial state and after annealing.

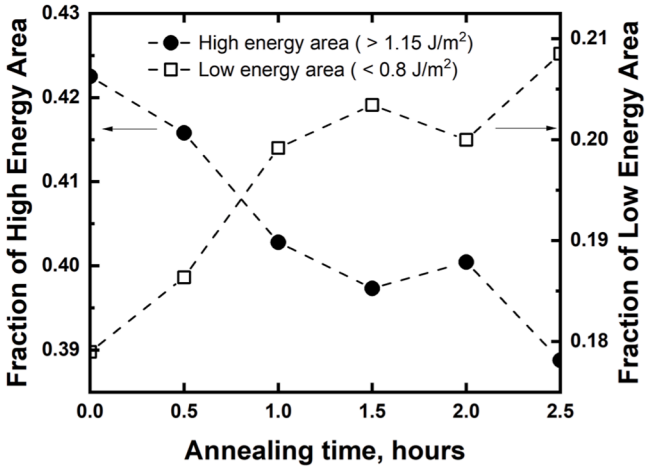

Fig. 3. The fractional area of high and low energy GBs as a function of annealing time.

energies. [36] Therefore, this represents the best available approximation that provides a comprehensive way to assign energies to the boundaries. As an example, Fig. 1 shows a meshed grain with its triangular elements colored by energy as assigned by the BRK function. With energies assigned in this way, we can determine the total energy of the GB network and how it changes with time.

The distribution of GB area as a function of GB energy in the initial and final states are compared in Fig. 2. For this graph, the energy range was divided into 11 discrete categories. In the observed microstructures, show a preference for lower energy states, with only 65% of the boundaries in states with energies between 1.0 and 1.4 J/m^2. Note also that the majority of boundaries below 0.7 J/m^2 are near the twin orientation. The important point here is that with annealing, the distribution shifts to lower energy; the lowest energy categories increase in relative area and the highest energy categories decrease in relative area. In fact, the average energy per area of the network decreases from 1.026 J/m^2 to 0.998 J/m^2 during annealing.

The increasing relative area of low energy boundaries and the decreasing relative area of high energy GBs at each annealing state are depicted in Fig. 3. The fractional area of GBs with energy less than 0.8 J/m^2 increases from about 18% of the total to 21%. At the same time, the fractional area of GBs with energy greater than 1.15 J/m^2 decreases from about 42% of the total to 39%. We note that the observed replacement of high energy GBs with lower energy GBs is consistent with

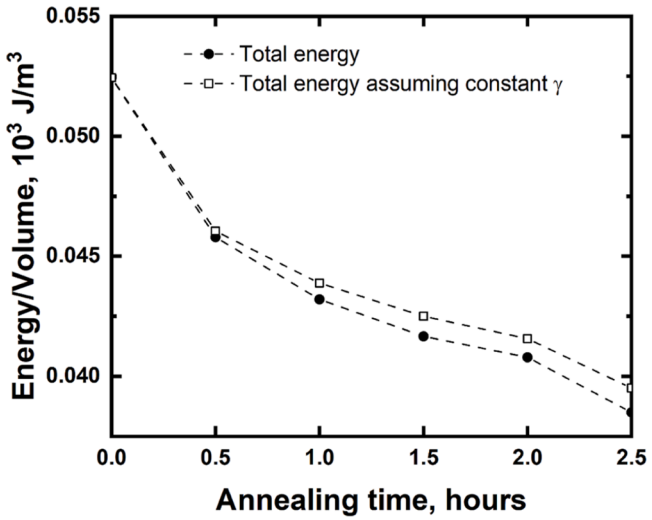

Fig. 4. The total GB energy per volume. The data represented by empty squares is computed under the assumption that every GB has the average GB energy of the initial state. Because of this constant energy assumption, energy reduction can only occur through GB area reduction. The data represented by solid circles is computed by assigning the BRK energies to each GB in each state. Although the areas are identical in the two cases compared, the GB network in the final state with anisotropic energies has a reduced average energy because of changes in the GB character distribution.

the model for the development of anisotropic GB character distributions. [11,37]

As grain growth proceeds, energy is dissipated both through the loss of area and the change in the types of GBs. The two energy dissipation mechanisms occur in a cooperative way so it is difficult to separate them. However, we can quantify the minimum amount of energy dissipated by changing the types of GBs. Fig. 4 compares the total excess GB energy per volume calculated using a constant average GB energy to the energy calculated using the anisotropic BRK function. It is clear from this comparison that when the change in the average grain boundary energy is accounted for, the actual energy dissipated is greater than explained by the change in area alone. Using the data in Fig. 4, the total energy change is 0.014 J/m^3 and the difference between the energy lost under the constant energy assumption and the anisotropic energies is 0.001 J/m^3. Based on this, we conclude that changes in the grain boundary character distribution decreased the energy by at least 7%.

The evidence presented so far has been based on system averages. Because low energy GBs are growing at the expense of higher energy boundaries, it is possible to find individual examples of this phenomenon. One such example is shown in Fig. 5. Here, a low energy GB (this is a low angle GB with a misorientation of 8.1° around [$\overline{0.49}$ 0.41 0.77], an axis that is about 5° from the [$\bar{1}$12] direction) increases in area in each time step at the expense of neighboring higher energy GBs. Tracking the change in energy that results from the motion of individual GBs was not possible. The challenge is that as a boundary moves and changes area, there are area and energy changes for all of the connected boundaries and it is unclear how to assign these changes to individual GBs. The low energy GB in Fig. 5 provides an excellent example; it is increasing in area at each time step, so its total energy is increasing. However, this is offset by the reduction in the areas of the surrounding higher energy boundaries. While these changes can be computed, it is not at all clear what fraction of the energy reduction of adjoining faces should be assigned to the low energy boundary of interest. Keep in mind that each boundary is terminated by (on average) five triple lines so that when it moves or changes area, ten other boundaries must also adjust their area, position, or orientation. There is no obvious way to distribute these changes among the affected boundaries. So, while it is not clear how to evaluate the energy dissipated by individual boundaries, the energy of the entire polycrystal can be measured and is clearly evolving in a way that lowers the average GB energy with time.

While it is well established that GBs in bicrystals migrate toward their centers of curvature, recent experimental observations [5,6] and simulations [38] (assuming anisotropic energies) of polycrystals find that curvature is not an accurate predictor for the direction or velocity of GB migration. We have shown here that during grain growth, higher energy GBs are substituted by lower energy GBs and this reduction in the energy per volume need not be connected to a negative change in area. In other words, this energy dissipation mechanism provides a driving force for the migration of GBs that does not depend on curvature, and we assert that this contributes to the absence of a correlation between measured GB velocity and curvature. Conversely, this mechanism is not operative in bicrystals with a single GB, so the fact that boundaries in bicrystals always migrate towards their center of curvature does not contradict the proposed boundary replacement mechanism.

The energy dissipated by the GB replacement process is evaluated to be at least 7% of the total. This is energy dissipated in spite of the fact that many of the boundaries are not moving in the direction predicted by curvature. There are other features of GB migration in polycrystalline Ni that might also play a role in disrupting the expected curvature-velocity correlation. For example, there are many twin boundaries in Ni. These boundaries are singular and their migration is not governed by curvature. [39] Furthermore, because the energy is anisotropic in the GB plane orientation space, the GB stiffness may have a significant effect on GB migration. [40,41] While it is not yet possible to judge the importance these contributions, it is clear that the average GB energy is decreasing with grain growth and this provides an energy dissipation mechanism that is not related to curvature.

In summary, using the BRK GB energy function for Ni together with three-dimensional microstructure data, we have evaluated the changes in the GB energy as a function of microstructure evolution. The average GB energy is decreasing with time by the process of GB replacement, in which higher energy GBs are replaced by lower energy boundaries. This dissipates GB energy by a mechanism that is unconnected to GB curvature and provides an explanation for the absence of a correlation between velocity and curvature in polycrystals.

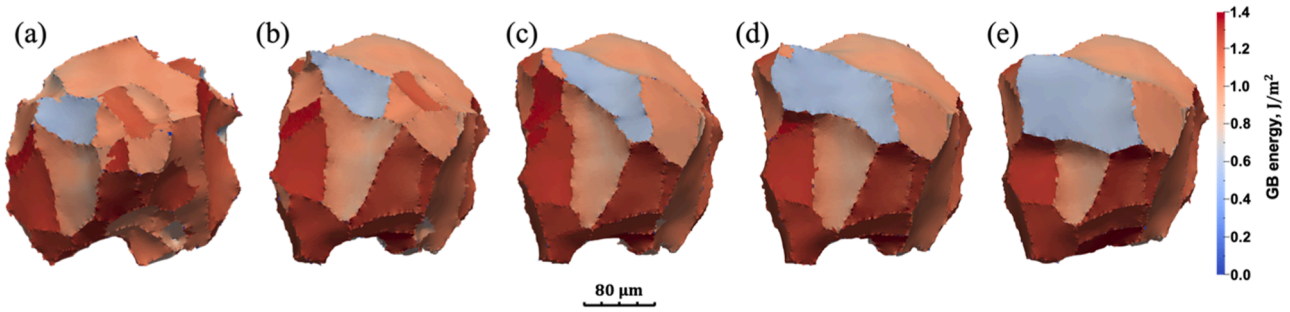

Fig. 5. Selected grain with faces colored by the GB energy at (a) the initial point and after (b) 30 min, (c) 1 h, (d) 1.5 h, and (e) 2.5 h.

Declaration of Competing Interest

The authors declare that they have no known competing financial interests or personal relationships that could have appeared to influence the work reported in this paper.

Acknowledgments

This work was supported by the National Science Foundation under DMREF Grant No. 2118945. The measurements were supported by the National Science Foundation under Grant No. DMR-0805100 and were carried out at the Advanced Photon Source which is a US Department of Energy (DOE) Office of Science User Facility operated for the DOE Office of Science by Argonne National Laboratory under contract no. DE-AC02–06CH11357. We would like to acknowledge the extensive contributions of Ulrich Lienert to the development of the measurement technique. F.A. would like to acknowledge support from NSF Grant No. 2114832.

References

[1] J.E. Burke, D. Turnbull, Recrystallization and grain growth, Prog. Metal Phys. 3 (1952) 220–292, https://doi.org/10.1016/0502-8205(52)90009-9.
[2] M. Hillert, On theory of normal and abnormal grain growth, Acta Metall. 13 (1965) 227–238, https://doi.org/10.1016/0001-6160(65)90200-2.
[3] G. Gottstein, D.A. Molodov, L.S. Shvindlerman, Grain boundary migration in metals: recent developments, Interface Sci. 6 (1998) 7–22, https://doi.org/10.1023/a:1008641617937.
[4] M. Upmanyu, R.W. Smith, D.J. Srolovitz, Atomistic simulation of curvature driven grain boundary migration, Inter. Sci. 6 (1998) 41–58.
[5] A. Bhattacharya, Y.F. Shen, C.M. Hefferan, S.F. Li, J. Lind, R.M. Suter, C.E. Krill, G. S. Rohrer, Grain boundary velocity and curvature are not correlated in Ni polycrystals, Science 374 (2021) 189–193, https://doi.org/10.1126/science.abj3210.
[6] V. Muralikrishnan, H. Liu, L. Yang, B. Conry, C.J. Marvel, M.P. Harmer, G. S. Rohrer, M.R. Tonks, R.M. Suter, C.E. Krill, A.R. Krause, Observations of unexpected grain boundary migration in $SrTiO_3$, Scripta Mater. 222 (2023), 115055, https://doi.org/10.1016/j.scriptamat.2022.115055.
[7] J. Zhang, W. Ludwig, Y.B. Zhang, H.H.B. Sorensen, D.J. Rowenhorst, A. Yamanaka, P.W. Voorhees, H.F. Poulsen, Grain boundary mobilities in polycrystals, Acta Mater. 191 (2020) 211–220, https://doi.org/10.1016/j.actamat.2020.03.044.
[8] C.S. Smith, Some elementary principles of polycrytalline microstructure, Metall. Rev. 9 (1964) 1–48, https://doi.org/10.1179/mtlr.1964.9.1.1.
[9] P.A. Beck. Interface migration in recrystallization. Metal Interfaces. American Society for Testing Materials, Cleveland, 1952. pp. 208–247.
[10] W.W. Mullins, 2-Dimensional motion of idealized grain boundaries, J. Appl. Phys. 27 (1956) 900–904.
[11] S.J. Dillon, G.S. Rohrer, Mechanism for the development of anisotropic grain boundary character distributions during normal grain growth, Acta Mater. 57 (2009) 1–7, https://doi.org/10.1016/j.actamat.2008.08.062.
[12] J. Gruber, D.C. George, A.P. Kuprat, G.S. Rohrer, A.D. Rollett, Effect of anisotropic grain boundary properties on grain boundary plane distributions during grain growth, Scr. Mater. 53 (2005) 351–355, https://doi.org/10.1016/j.scriptamat.2005.04.004.
[13] J. Gruber, H.M. Miller, T.D. Hoffmann, G.S. Rohrer, A.D. Rollett, Misorientation texture development during grain growth. Part I: simulation and experiment, Acta Mater. 57 (2009) 6102–6112, https://doi.org/10.1016/j.actamat.2009.08.036.
[14] J. Gruber, A.D. Rollett, G.S. Rohrer, Misorientation texture development during grain growth. Part II: theory, Acta Mater. 58 (2010) 14–19, https://doi.org/10.1016/j.actamat.2009.08.032.
[15] F.J. Humphreys, M. Hatherly Recrystallization and Related Annealing Phenomena, Elsevier, London, 1995.
[16] T. Watanabe, H. Fujii, H. Oikawa, K.I. Arai, Grain boundaries in rapidly solidified and annealed Fe-6.5 mass% Si polycrystalline ribbons with high ductility, Acta Metallurgica 37 (1989) 941–952, https://doi.org/10.1016/0001-6160(89)90021-7.
[17] A.I. Barg, E. Rabkin, W. Gust, Faceting transformation and energy of a sigma-3 grain-boundary in silver, Acta Metall. Mater. 43 (1995) 4067–4074, https://doi.org/10.1016/0956-7151(95)00094-c.
[18] T.G. Ference, R.W. Balluffi, Observation of a reversible grain-boundary faceting transition induced by changes of composition, Scripta Metall. 22 (1988) 1929–1934, https://doi.org/10.1016/s0036-9748(88)80240-0.
[19] P.J. Goodhew, T.Y. Tan, R.W. Balluffi, Low-energy planes for tilt grain-boundaries in gold, Acta Metall. 26 (1978) 557–567.
[20] R. Hadian, B. Grabowski, M.W. Finnis, J. Neugebauer, Migration mechanisms of a faceted grain boundary, Phys. Rev. Mater. 2 (2018), https://doi.org/10.1103/PhysRevMaterials.2.043601.
[21] C. Herring, Some theorems on the free energies of crystal surfaces, Phys. Rev. 82 (1951) 87–93, https://doi.org/10.1103/PhysRev.82.87.
[22] T.E. Hsieh, R.W. Balluffi, Observations of roughening de-faceting phase-transitions in grain-boundaries, Acta Metall. 37 (1989) 2133–2139, https://doi.org/10.1016/0001-6160(89)90138-7.
[23] T. Muschik, W. Laub, U. Wolf, M.W. Finnis, W. Gust, Energetic and kinetic aspects of the faceting transformation of a sigma-3-grain-boundary in Cu, Acta Metall. Mater. 41 (1993) 2163–2171, https://doi.org/10.1016/0956-7151(93)90386-7.
[24] R.L. Fullman, J.C. Fisher, Formation of annealing twins during grain growth, J. Appl. Phys. 22 (1951) 1350–1355, https://doi.org/10.1063/1.1699865.
[25] P.J. Goodhew, Annealing twin formation by boundary dissociation, Metal. Sci. 13 (1979) 108–112.
[26] B. Lin, Y. Jin, C.M. Hefferan, S.F. Li, J. Lind, R.M. Suter, M. Bernacki, N. Bozzolo, A. D. Rollett, G.S. Rohrer, Observation of annealing twin nucleation at triple lines in nickel during grain growth, Acta Mater. 99 (2015) 63–68, https://doi.org/10.1016/j.actamat.2015.07.041.
[27] L.E. Murr, Energetics of grain-boundary triple junctions and corner-twinned junctions - transmission electron microscope studies, J. Appl. Phys. 39 (1968), https://doi.org/10.1063/1.1656013, 5557-&.
[28] J.W. Cahn, D.W. Hoffman, Vector thermodynamics for anisotropic surfaces 2. Curved and faceted surfaces, Acta Metall. 22 (1974) 1205–1214.
[29] D.W. Hoffman, J.W. Cahn, Vector thermodynamics for anisotropic surfaces 1. Fundamentals and application to plane surface junctions, Surf. Sci. 31 (1972) 368–388.
[30] G.S. Rohrer, Grain boundary energy anisotropy: a review, J. Mater. Sci. 46 (2011) 5881–5895, https://doi.org/10.1007/s10853-011-5677-3.
[31] A. Bhattacharya, Y.F. Shen, C.M. Hefferan, S.F. Li, J. Lind, R.M. Suter, G.S. Rohrer, Three-dimensional observations of grain volume changes during annealing of polycrystalline Ni, Acta Mater. 167 (2019) 40–50, https://doi.org/10.1016/j.actamat.2019.01.022.
[32] C.M. Hefferan, S.F. Li, J. Lind, U. Lienert, A.D. Rollett, P. Wynblatt, R.M. Suter. Statistics of High Purity Nickel Microstructure From High Energy X-ray Diffraction Microscopy, Cmc-Computers Materials & Continua 14 (2009) 209–219.
[33] M.A. Groeber, M.A. Jackson. DREAM.3D: a Digital Representation Environment for the Analysis of, Microstructure in 3D, 2014, 3:5, Integrating Materials and Manufacturing Innovation 3 (2014) 5.
[34] V.V. Bulatov, B.W. Reed, M. Kumar, Grain boundary energy function for fcc metals, Acta Mater. 65 (2014) 161–175, https://doi.org/10.1016/j.actamat.2013.10.057.
[35] D.L. Olmsted, S.M. Foiles, E.A. Holm, Survey of computed grain boundary properties in face-centered cubic metals: I. Grain boundary energy, Acta Mater. 57 (2009) 3694–3703, https://doi.org/10.1016/j.actamat.2009.04.007.
[36] G.S. Rohrer, E.A. Holm, A.D. Rollett, S.M. Foiles, J. Li, D.L. Olmsted, Comparing calculated and measured grain boundary energies in nickel, Acta Mater. 58 (2010) 5063–5069, https://doi.org/10.1016/j.actamat.2010.05.042.
[37] G. Rohrer, J. Gruber, A.D. Rollett. A model for the origin of anisotropic grain boundary character distributions in polycrystalline materials. in: Rollett AD, (Ed.). Materials Processing and Texture, vol. 201. J. Wiley and Sons, Hoboken, NJ, 2009. pp. 343–354.
[38] S. Florez, K. Alvarado, B. Murgas, N. Bozzolo, D. Chatain, C.E. Krill, M.Y. Wang, G. S. Rohrer, M. Bernacki, Statistical behaviour of interfaces subjected to curvature flow and torque effects applied to microstructural evolutions, Acta Mater. 222 (2022), 117459, https://doi.org/10.1016/j.actamat.2021.117459.
[39] C. Herring. The Use of Classical Macroscopic Concepts in Surface Energy Problems. in: Gomer R, Smith CS, (Eds.). Structure and Properties of Solid Surfaces; Proceedings of a Conference Arranged By the National Research Council and Held in September 1952, in Lake Geneva, Wisconsin, USA. University of Chicago Press, Chicago, 1953. pp. 5–81.
[40] F. Abdeljawad, S.M. Foiles, A.P. Moore, A.R. Hinkle, C.M. Barr, N.M. Heckman, K. Hattar, B.L. Boyce, The role of the interface stiffness tensor on grain boundary dynamics, Acta Mater. 158 (2018) 440–453, https://doi.org/10.1016/j.actamat.2018.06.025.
[41] R.D. Moore, T. Beecroft, G.S. Rohrer, C.M. Barr, E.R. Homer, K. Hattar, B.L. Boyce, F. Abdeljawad, The grain boundary stiffness and its impact on equilibrium shapes and boundary migration: analysis of the Sigma 5, 7, 9, and 11 boundaries in Ni, Acta Mater. 218 (2021), 117220, https://doi.org/10.1016/j.actamat.2021.117220.